JOURNAL OF VIROLOGY, Mar. 1983, p. 1118–1139
0022-538X/83/031118-22$02.00/0
Copyright © 1983, American Society for Microbiology
Vol. 45, No. 3

Coliphage P1 Morphogenesis: Analysis of Mutants by Electron Microscopy

JEAN T. WALKER AND DONALD H. WALKER, JR.*
Department of Microbiology, University of Iowa, Iowa City, Iowa 52242

Received 1 July 1982/Accepted 19 October 1982

We used electron microscopy and serum blocking power tests to determine the phenotypes of 47 phage P1 amber mutants that have defects in particle morphogenesis. Eleven mutants showed head defects, 30 showed tail defects, and 6 had a defect in particle maturation (which could be either in the head or in the tail). Consideration of previous complementation test results, genetic and physical positions of the mutations, and phenotypes of the mutants allowed assignment of most of the 47 mutations to genes. Thus, a minimum of 12 tail genes, 4 head genes, and 1 particle maturation gene are now known for P1. Of the 12 tail genes, 1 (gene 19, located within the invertible C loop) codes for tail fibers, 6 (genes 3, 5, 16, 20, 21, and 26) code for baseplate components (although one of these genes could code for the tail tube), 1 (gene 22) codes for the sheath, 1 (gene 6) affects tail length, 2 (genes 7 and 25) are involved in tail stability, and 1 (gene 24) either codes for a baseplate component or is involved in tail stability. Of the four head genes, gene 9 codes for a protein required for DNA packaging. The function of head gene 4 is unclear. Head gene 8 probably codes for a minor head protein, whereas head gene 23 could code for either a minor head protein or the major head protein. Excluding the particle maturation gene (gene 1), the 12 tail genes are clustered in three regions of the P1 physical genome. The four head genes are at four separate locations. However, some P1 head genes have not yet been detected and could be located in two regions (for which there are no known genes) adjacent to genes 4 and 8. The P1 morphogenetic gene clusters are interrupted by many genes that are expressed in the prophage.

Coliphage P1 consists of an icosahedral, DNA-containing head and a complex tail (47; Fig. 1). The tail has a tube surrounded by a contractile sheath. At the distal end of the sheath is an ill-defined baseplate to which kinked tail fibers (probably six) are attached. At the proximal end of the sheath is a cap (occasionally seen on tails unattached to heads). The head is attached to the tail via a neck which protrudes from a vertex of the head (47). The neck is attached to the head via a head-neck connector (which is only seen when the head is empty or has been disrupted).

One of the unique characteristics of P1 is that it normally produces isometric heads of at least three different sizes (P1B, P1S, and P1M, having diameters of 86, 65, and 47 nm, respectively [47]). As part of an approach to determine how the different head sizes are assembled, we examined 103 P1 amber mutants to identify those defective in head structure.

A genetic map for P1 (Fig. 2), which includes these 103 amber mutations, has been established (49). Two-factor crosses permitted assignment of the mutations into 10 linear arrays, or linkage clusters, I through X, with mutations in cluster X behaving as two subgroups, X-1 and X-2. However, cistron designations, apart from those originally assigned by Scott (39), were not assigned because complementation tests in liquid frequently gave ambiguous results.

With other phages, amber mutants can be divided into two major classes depending on whether they have a gene defective in a function which is required early or one which is required late in phage particle development. Late genes are involved in particle morphogenesis (e.g., production of proteins which become structural components of the particle) or in cell lysis. Generally, early gene mutants (i.e., those defective in regulation of transcription, DNA synthesis, or recombination) do not allow synthesis of any of the late gene products, including those causing lysis. Thus, those mutants that cause cell lysis should have morphological defects. Therefore, we determined which of the 103 P1 amber mutants could cause cell lysis (50) and examined 55 of them by electron microscopy for

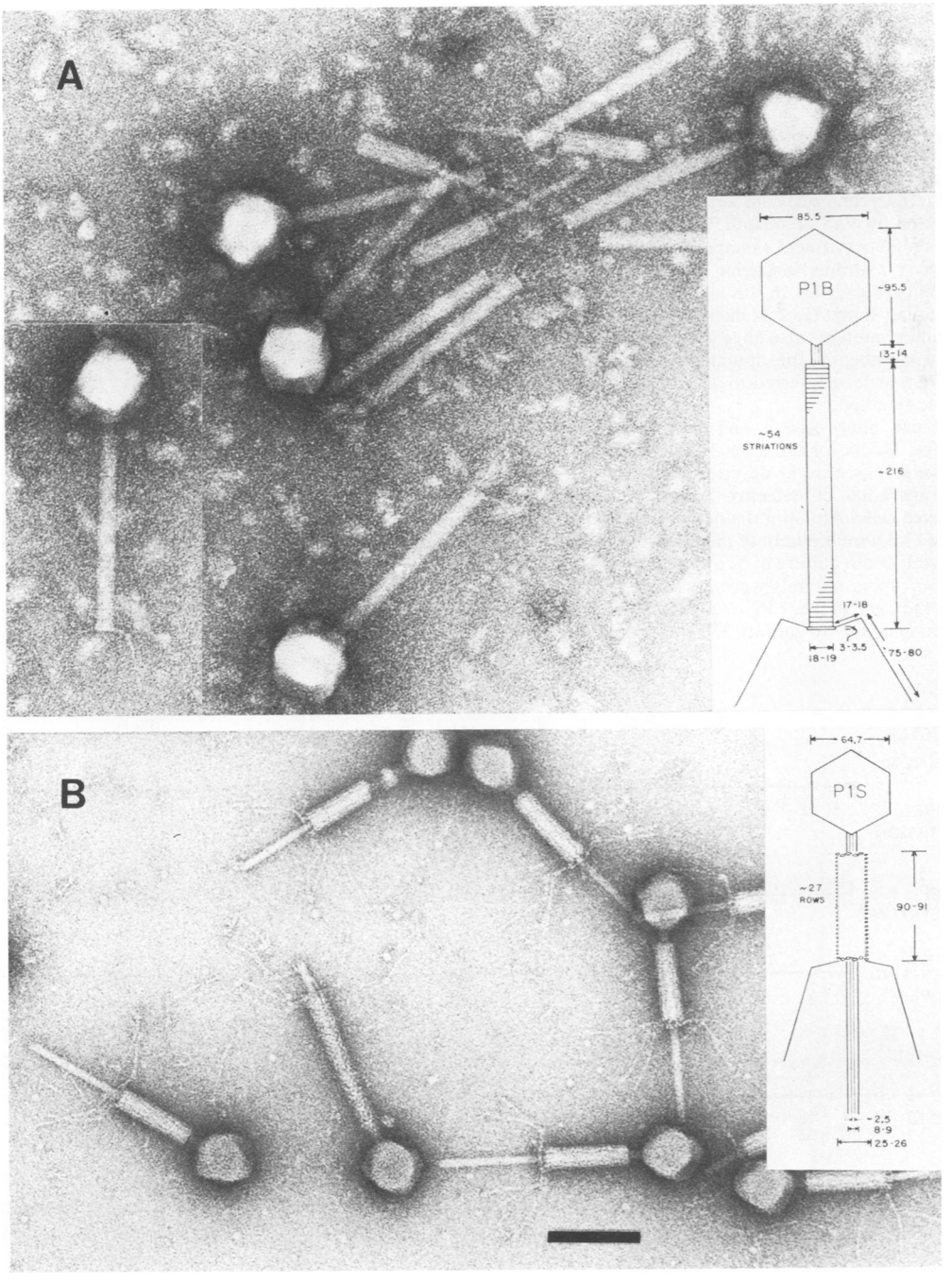

FIG. 1. Micrographs showing normal P1 particles. (A) Lysate of P1 *vir* · Sh has big heads (P1B), full of DNA, and tails, the majority of which have sheaths. (B) Particles from a CsCl gradient. The full small heads (P1S) have tails with sheaths in varying stages of contraction; baseplates and tail fibers can be easily seen. Insets show diagrammatic scale drawings of P1; dimensions are in nanometers. Bar, 100 nm.

structural defects (this paper). In doing so, we identified those mutants whose defects are in early functions, in lysis functions, and in head and tail morphology. In addition, because the genetic (39, 50) and physical (21, 34, 38, 43, 45) locations of these mutations on the P1 genome

are known, we determined the extent of clustering of the functions represented by these mutants.

MATERIALS AND METHODS

Bacterial and phage strains. Bacterial strains were *Shigella dysenteriae sup*^{0} strains Sh-15 and Sh-16 (which is a streptomycin-resistant Sh-15 strain) (5) and the tetracycline-resistant *sup*$^+$ strain Sh-16*supF* constructed by Van Montagu (50). Phage strains were P1 *vir* (the supervirulent mutant P1 *kcvir*^{s} of Sarkar that grows on strains lysogenic for P1 [39]), P1 amber mutants (Fig. 2) 13, 16, 19, and 21 of Scott (39), and 51 P1 amber mutants of Walker and Walker (49). These P1 amber mutants also have the *vir* mutation (i.e., they are *vir* amber double mutants); for simplicity these mutants will be referred to as *am*13, etc., without the *vir* designation.

Media, phage assays, and the preparation of phage stocks. Media, phage assays, and the preparation of phage stocks were as described previously (50).

Preparation of defective lysates of amber phage-infected cells. At 0 min the desired amber mutant was added (at a multiplicity of infection of 4 to 6) to a log-phase L-broth culture of *S. dysenteriae sup*^{0} strain Sh-15. *vir* amber mutants were used to avoid lysogenization (32), and amber$^+$ P1 *vir* was included as a control. After allowing 10 min at 37°C for adsorption in the presence of 5 mM $CaCl_2$, the culture was filtered to remove unadsorbed phage, diluted 2.5-fold in fresh medium containing 5 mM $MgSO_4$, and incubated at 37°C with vigorous shaking. With the onset of lysis (usually at 60 to 70 min when it occurred), DNase and RNase were added to final concentrations of 1 μg/ml. At 110 min, when lysis was complete, a sample of the lysate was prepared immediately for electron microscopy as described below, and the lysate was assayed, with *sup*^{0} and *sup*$^+$ strains Sh-16 and Sh-16 *supF*, for viable phage and revertants. Under these conditions titers for mutants on *sup*$^+$ cells were lower by a factor of 10^4 than those obtained using a P1 *vir* lysate as a control. This is comparable to results obtained for T4 (55) and P2 (32). Such titers for mutants are due primarily to transmission of ambers.

The remaining lysate was chilled, and 5 ml was centrifuged (at 35,000 rpm for 2 s at 4°C in an SW50.1 rotor) to pellet unlysed cells and cell debris. The supernatant fluids were centrifuged (at 22,000 rpm for 2 h in the same rotor) to pellet any phage components present. The pellet was left at 4°C for 2 days to resuspend in 0.25 ml of culture fluid (i.e., a 20-fold concentration of phage components), and a sample was prepared for electron microscopy.

Serum blocking assays. Those defective lysates used for electron microscopy were also assayed for serum blocking antigen (SBA). The method for determining

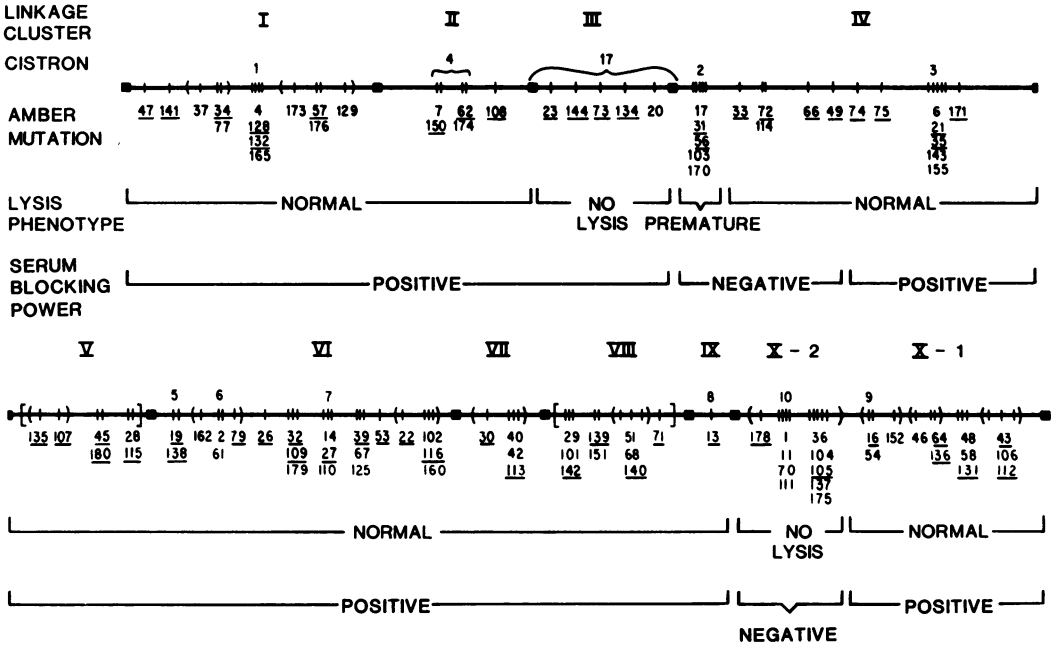

FIG. 2. Genetic map of P1 amber mutations, modified from Walker and Walker (50), showing results of host cell lysis and serum blocking power tests. Regions demarcating the 10 linkage clusters are represented by solid blocks. The cistron designations above the map line include the original 1 to 10 of Scott (39) and 17 of Walker and Walker (50). Groups of amber mutations vertically stacked under very close hash marks or within parentheses do not show complementation (49). The orientation of groups of amber mutations within parentheses or within brackets with respect to mutations outside these groups is unknown. The spacing of the hash marks is not meant to indicate either genetic or physical distance. Underlined mutations indicate the mutants that were used in the experiments reported in this paper.

SBA was a modification of the DeMars (9) method as used by Israel et al. (22) for P22 and Ward et al. (52) for T4; it compares rates rather than final levels of serum inactivation by blocking antigens.

Serial twofold dilutions were made of the lysates after they had been treated with chloroform for 20 min at 37°C to kill any viable cells. Cells infected with mutants (in linkage clusters III and X-2; Fig. 2) that do not cause cell lysis were lysed by sonication at the time when lysis occurred with amber$^+$-infected cells. Cells infected with other mutants and with P1 *vir* were not sonicated, except as described below for P1 *vir*, to obtain a standard curve. Reaction mixtures contained 0.45 ml of a lysate dilution and 0.1 ml of tester phage, to which was subsequently added 0.45 ml of antiphage serum. The tester phage was P1 *kc* at a final concentration of 3×10^5 PFU/ml; the turbid plaques could be distinguished from the clear plaques of any revertants present in the P1 *vir* amber lysates. The first-order rate constant (k) for phage inactivation of the undiluted hyperimmune serum at 37°C was 1,500 min^{-1}. This serum had a k of 0.1 min^{-1} in the final dilution of the reaction mixture. The reaction mixtures were assayed (on strain Sh-16) for surviving tester phage at the end of 46 min, when tester phage survival was about 1% in the absence of SBA. This control without SBA was always included in each group of tests done on different days. This inactivation was assumed to be exponential throughout the 46-min incubation.

To obtain standard curves, lysates of amber$^+$ P1 *vir* grown on strain Sh-15 were used as SBA; the phage were inactivated by either sonication or UV treatment so the plaques would not obscure those of the competing P1 *kc* tester phage.

The results of the serum blocking assays were plotted as percent residual $k = (1 - k_{final}/k_{initial}) \times 100 = (1 - \ln S/S_d/\ln S/S_0) \times 100$, where S/S_0 = survival of the tester phage in the control after 46 min with serum but no SBA, and S/S_d = survival of the tester phage after 46 min with both serum and SBA at dilution d of the latter. Rather than showing graphs for the 55 mutants tested, comparisons were made using the dilution at which residual $k = 50\%$.

Electron microscopy. A 0.4-ml sample of concentrated or unconcentrated lysate of the phage-infected cells was dialyzed for 15 min by placing it on a membrane filter (Millipore Corp.; average pore size, 25 nm) floating on P1 buffer (rather than water, which caused head disruption). This dialysis was done at room temperature to decrease tail contractions obtained by dialysis at 4°C. A drop of sample was placed on a glow-discharged, carbon-coated, 400-mesh copper grid and allowed to stand for 2 min. A small drop of sodium phosphotungstate (1%; pH 7.0) was added and left for 30 s before the excess liquid was removed with filter paper. A JEOL 100B electron microscope with an anticontamination device was used at 80 kV. Micrographs were taken at initial magnifications of 10,000 to 50,000 on Kodak 4463 film.

RESULTS

We examined, by electron microscopy, lysates of 55 P1 amber mutants grown under nonpermissive conditions to determine their phenotypes. In such lysates, mutants defective in some aspect of tail assembly should produce normal heads and one of a variety of tail component combinations. Similarly, mutants defective in some aspect of head assembly should produce normal tails and either no heads or one of a variety of defective head structures. In addition, we used serum blocking assays to detect the presence of tail fibers in the defective lysates.

Of 103 P1 amber mutants previously tested for lysis of nonpermissive cells (50), 83 caused cell lysis at the normal lysis time for P1. These 83 mutations are in linkage clusters (Fig. 2) I, II, V, VI, VII, VIII, and IX and parts of IV and X (i.e., X-1). By analogy with other phages, these mutants would be defective in late genes involved in particle morphogenesis.

The number of cistrons represented by these 83 mutants is unknown. Therefore, 47 mutants (underlined in Fig. 2) were chosen for study by electron microscopy from the maximum possible number of cistrons in the following way. These 47 mutants represent (i) at least one mutation from each of the groupings of mutations (shown in Fig. 2 as vertically stacked under very close hash marks or within parentheses) that had been found (49) not to show complementation and (ii) each of the single mutations outside these groupings. In addition, eight mutants (also underlined in Fig. 2), representing those that cannot cause cell lysis (linkage clusters III and X-2) or that cause premature cell lysis (linkage cluster IV), were also included in this study.

Serum blocking assays. P1 tail fibers are only 1 to 2 nm in thickness (47) and so are only seen by electron microscopy when they are attached to phage particles and when the staining conditions are such as to give optimal contrast between the fibers and the background (Fig. 1). Therefore, because in other phages with contractile tails, such as T4, the majority of SBA can be attributed to tail fibers, serum blocking assays were done to confirm the presence of attached fibers or to detect the presence of unattached fibers in the P1 defective lysates. Results were plotted as percent residual k versus lysate dilution as described above, and the dilution giving 50% residual k was determined for each defective lysate. These dilutions were designated SBA values.

As would be expected for a phage such as P1 that has a complex morphology and therefore would code for various structures in addition to tail fibers, the majority of mutants showed significant serum blocking power (similar to that of the control P1 *vir* lysates), indicating that tail fibers were present (Table 1; Fig. 2).

Those mutants that gave negative results (i.e., SBA values of less than 1) have mutations in linkage cluster X-2 and part of cluster IV. Because cluster X-2 mutants did not lyse the host

cells, these lysates were tested for SBA both before and after sonication to cause cell lysis; negative results were obtained in both instances, indicating that these negative results were not due to a failure of the cells to lyse. (Mutants in cluster III also did not lyse the host cells, but gave positive SBA results, indicating that sonication does not adversely affect SBA activity.) Cluster X-2 mutations have been shown to be in the same cistron (cistron 10), and mutants representing this cistron are probably defective in the expression of late genes (50). Since SBAs are late gene products, this would explain why negative results are obtained with defective lysates of these mutants.

All of those mutants (74, 75, 21, 35, and 171) located in the right part of linkage cluster IV gave normal levels of SBA. However, mutants (31, 56, 33, 72, 66, and 49) located in the left part of cluster IV gave negative SBA results (i.e., SBA values of less than 1), indicating that these mutants produce few, if any, tail fibers. The significance of these results obtained with the latter six mutants is discussed in the next section.

Serum blocking assays confirmed electron microscopic examination (see below) of the mutants in the cases in which normal amounts of sheathed tails were produced. That is, tail fibers were seen by electron microscopy on particles produced by all of the mutants that produced normal amounts of sheathed tails (either extended or contracted), except mutants 128, 150, 33, 72, 66, and 138. The preparations of mutants 128, 150, and 138 were not good enough to determine the presence of tail fibers, but these mutants all showed serum blocking power, and for each there are allelic mutants (i.e., mutants that did not show complementation [49]) where tail fibers could be seen. Therefore, these mutants are presumed to have tail fibers attached to their tails. Preparations of mutants, 33, 72, and 66 in linkage cluster IV were good enough to detect any tail fibers if present, and these mutants did not show serum blocking power, confirming that these mutants do not produce tail fibers.

SBA was produced by all mutants (except *am*49; see next section) that did not produce sheathed tails (and where tail fibers therefore could not be detected by electron microscopy), indicating that tail fibers were made even though no sheathed tail was available for their attachment.

Electron microscopy of P1 amber mutants. Defective lysates of the 55 mutants were examined by electron microscopy before, as well as after, differential centrifugation to concentrate any phage structures present. Amber$^+$ P1 *vir* controls (Fig. 1) prepared at the same time as the defective lysates were examined in parallel. The types of phage structures seen before and after centrifugation were similar except that where unattached tails had sheaths which had slipped down from the top of the tail before centrifugation (mutants in cluster VII and the right part of VI; see below), there was a decrease in the proportion of tails relative to polysheath after centrifugation. This decrease is probably caused by the sheath subunits dissociating from the tail tubes after centrifugation and polymerizing to form polysheath during resuspension of the centrifuged pellet at 4°C for 2 days, conditions which allow sheath subunits to polymerize in T4 (1). Where tails (either attached to or free from heads) had extended sheaths before centrifugation, the majority had contracted or semicontracted sheaths after the concentration steps. Lysates which showed full heads before centrifugation showed full heads after centrifugation if the heads were attached to tails. However, a high proportion of empty heads were seen after centrifugation if the full heads were not attached to tails before centrifugation. Results are summarized in Table 1 and Fig. 17.

Mutations affecting tail assembly. Mutations affecting tail assembly are located in linkage clusters IV through VIII. Each tail-defective mutant produces complete heads. The heads of mutants 33, 72, and 66 (in linkage cluster IV) are attached to tails which are complete except that they are missing tail fibers (Fig. 3). These mutants do not show serum blocking power, which confirms that fibers are not present either attached or unattached to the particles. However, it is unclear whether the whole tail fiber is missing or just the distal portion, because short projections, which could be part of the baseplate, are occasionally seen protruding from the base of the sheath, and the serum blocking assays did not distinguish between these possibilities. Therefore, it remains unknown whether the kinked P1 tail fiber is made of more than one polypeptide and whether the mutations of mutants 33, 72, and 66 are in the same gene.

Mutants 49, 74, 75, 21, 35, and 171 in cluster IV and mutants 135, 107, and 45 in cluster V produce complete heads and polysheath (Fig. 4). In T4 phage, completed baseplates are required for the tube polypeptide to initiate polymerization to form the tube, and then the sheath polypeptide polymerizes around the tube to form the tail (26). However, unlike the tube polypeptide, the sheath polypeptide can polymerize by itself to form polysheath. Therefore, the presence of polysheath alone means that the defect is in the baseplate, whereas the presence of polysheath and baseplates means that the defect is in the tube (or baseplate, if the defect has not damaged the structural integrity of the

TABLE 1. Phenotypic classification of P1 amber mutants

Mutant no.	Linkage cluster[a]	Host lysis[b]	SBP[c]	Phage structures[d]	Probable defect	Gene[e]
47	I	+	4.1	CP with EH + UsT	Particle maturation	1
141	I	+	3.2	CP with EH + UsT	Particle maturation	1
34	I	+	3.8	CP with EH + UsT	Particle maturation	1
128	I	+	3.3	CP with EH + UsT	Particle maturation	1
132	I	+	7.5	CP with EH + UsT	Particle maturation	1
57	I	+	4.1	CP	Particle maturation	1
150	II	+	5.8	CT; EH, clumped	Head	4
62	II	+	3.4	CT; EH, clumped	Head	4
108	II	+	4.1	CT; EH, clumped	Head	4?
23	III	−	2.7	Rare CP	Lysis	17
144	III	−	ND	Rare CP	Lysis	17
73	III	−	ND	Rare CP	Lysis	17
134	III	−	ND	Rare CP	Lysis	17
31	IV	++	<1	Few CP	Lysis regulation	2
56	IV	++	<1	Few CP	Lysis regulation	2
33	IV	+	<1	CP without TF	Tail fiber	19?
72	IV	+	<1	CP without TF	Tail fiber	19
66	IV	+	<1	CP without TF	Tail fiber	19?
49	IV	+	<1	CH; PS	Baseplate or tube	20
74	IV	+	2.1	CH; PS	Baseplate or tube	20?
75	IV	+	3.0	CH; PS	Baseplate or tube	3
21	IV	+	2.3	CH; PS	Baseplate or tube	16
35	IV	+	4.1	CH; PS	Baseplate or tube	3
171	IV	+	2.5	CH; PS	Baseplate or tube	3
135	V	+	5.4	CH; PS	Baseplate or tube	21
107	V	+	3.7	CH; PS	Baseplate or tube	21
45	V	+	4.9	CH; PS	Baseplate or tube	21
180	V	+	2.6	CH; TT	Sheath	22
115	V	+	5.2	CT with HC	Head	23
19	VI	+	2.6	CP with FH + UsT (ST)	Baseplate	5
138	VI	+	5.6	CP with FH + UsT (ST)	Baseplate	5
79	VI	+	5.2	CH with short tail (PS)	Tail length	6
26	VI	+	4.1	CH; PS; US (TT)	Baseplate or tail stability	24
32	VI	+	4.3	CH; PS; US	Baseplate or tail stability	24
109	VI	+	4.9	CH; PS; US (ST; TT)	Baseplate or tail stability	24
27	VI	+	6.3	CH; TSS; US; PS (ST; TT)	Tail stability	7
39	VI	+	4.5	CH; TSS; US; PS (TT)	Tail stability	7
53	VI	+	2.0	CH; TSS; US; PS	Tail stability	7
22	VI	+	4.5	CH; TSS; US; PS (ST)	Tail stability	7
116	VI	+	3.4	CH; TSS; US; PS (ST; TT)	Tail stability	7
30	VII	+	3.7	CH; TSS; PS; CoT with PS	Tail stability	25
113	VII	+	4.9	CH; TSS; PS (CoT with PS)	Tail stability	25
142	VIII	+	5.9	CH; PS; CP with FH + UsT	Baseplate	26?
139	VIII	+	4.6	CH; PS	Baseplate or tube	26
140	VIII	+	5.8	CH; PS	Baseplate or tube	26
71	VIII	+	3.7	CH; PS	Baseplate or tube	26
13	IX	+	3.9	CT with HC; EH	Head	8
178	X-2	−	<1	Rare CP	Late gene expression	10
105	X-2	−	<1	Rare CP	Late gene expression	10
16	X-1	+	3.6	CT; EH	Head	9
64	X-1	+	5.5	CT; EH	Head	9
136	X-1	+	3.8	CT; EH	Head	9

TABLE 1—*Continued*

Mutant no.	Linkage cluster[a]	Host lysis[b]	SBP[c]	Phage structures[d]	Probable defect	Gene[e]
131	X-1	+	ND	CT; EH	Head	9
43	X-1	+	5.1	CT; EH	Head	9
112	X-1	+	5.9	CT; EH	Head	9

[a] See Fig. 2.

[b] Described in Walker and Walker (50). +, Lysis occurred; −, lysis did not occur; ++, lysis occurred prematurely.

[c] SBP, Serum blocking power, expressed as the defective lysate dilution giving 50% residual *k* (see text). ND, Not done.

[d] CH, Complete heads; CP, complete particles; CT, complete tails; CoT, contracted tails; EH, empty heads; FH, full heads; HC, head-neck connectors; PS, polysheath; ST, stacked tails; TF, tail fibers; TSS, tails with slipped sheaths; TT, tail tubes; US, unit-length sheaths; UsT, unstable tails (tails in various stages of contraction). Parentheses denote that few of these structures were seen (see text).

[e] Numbers up to 10 assigned by Scott (39); numbers 17 and 19 through 26 were assigned by Walker and Walker (50; this paper). Queries denote uncertain gene designations.

baseplate but only the ability of the tube to be built upon it.) The baseplate of P1 (Fig. 1) is much thinner than that of T4 and has not been seen unattached to the P1 particle; therefore, the defect of these cluster IV and V mutants could be in either baseplate or tube formation. In addition to this defect, *am*49 does not show serum blocking power, indicating that tail fibers are not produced. This mutation is located next to mutations 33, 72, and 66, where the only defect is tail fiber production; therefore, *am*49 may be polar on these mutations (see below).

In T4, at least 15 genes are involved in baseplate formation (53); therefore, if these nine P1 mutants (49, 74, 75, 21, 35, 171, 135, 107, and 45) are defective in baseplate formation, they may be defective in different components of the baseplate and represent several genes. In support of this is the fact that mutants 49, 74, 75, 21, 35, and 171 are in one linkage cluster (IV) and

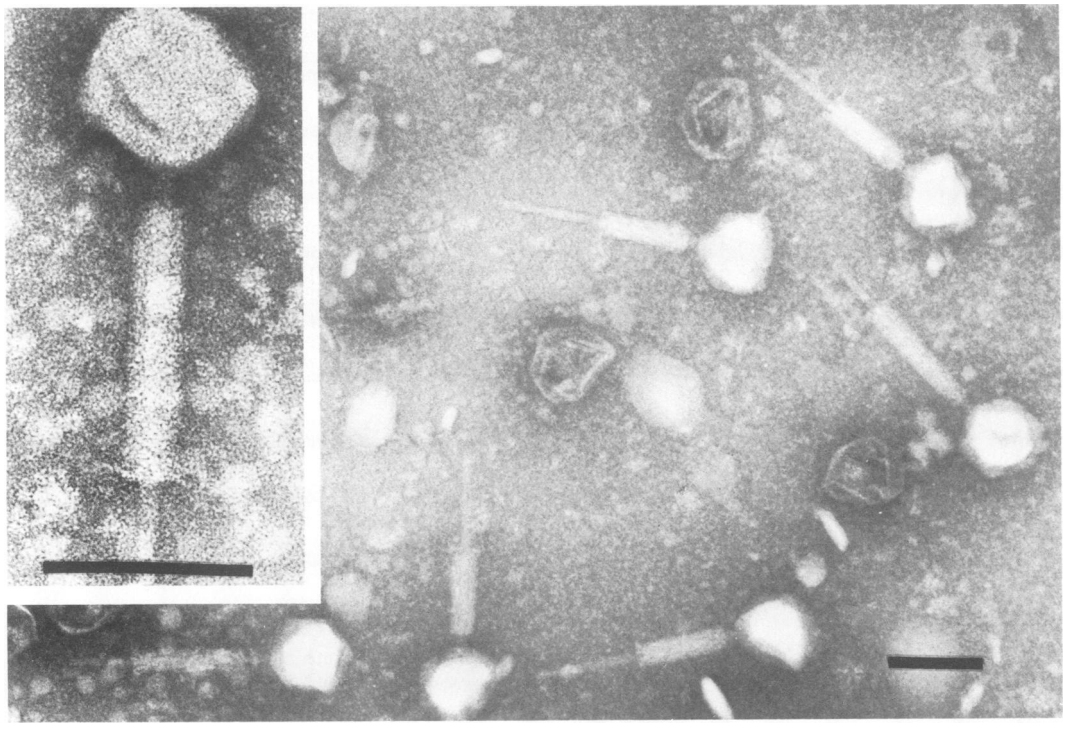

FIG. 3. Micrograph of P1 *am*66 defective lysate. Inset shows a single particle from P1 *am*72 defective lysate. All particles lack tail fibers. Contraction of sheaths is an artifact due to preparation procedures. Bars, 100 nm.

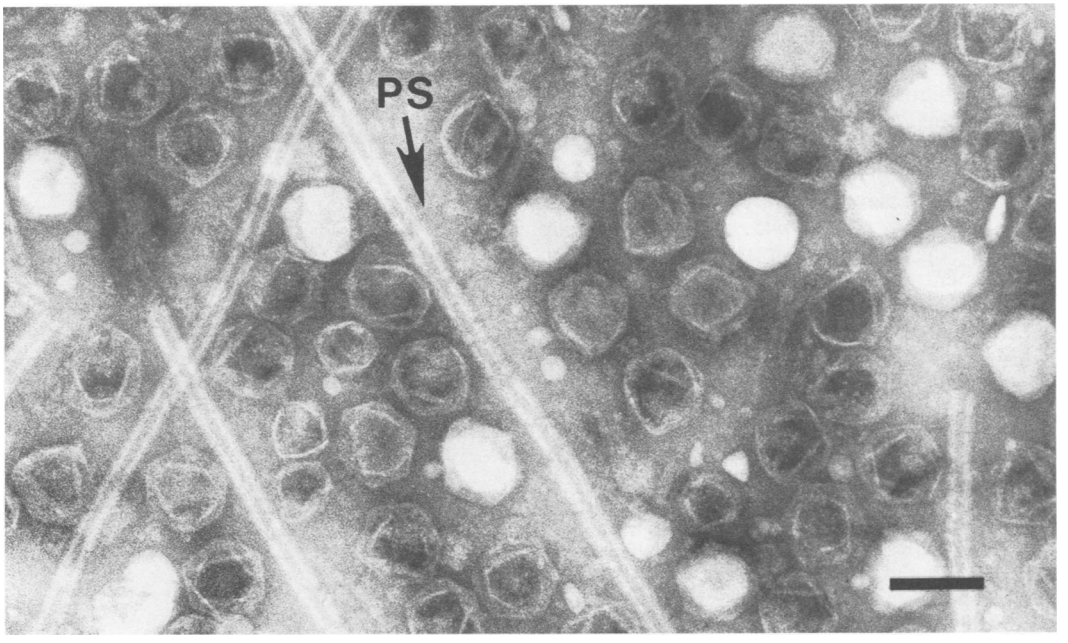

FIG. 4. Micrograph of P1 *am*35 defective lysate. This lysate is characterized by polysheath (PS) and normal heads, many of which are empty due to preparation procedures. Bar, 100 nm.

mutants 135, 107, and 45 are in another (V), and the restriction fragments that rescue these two groups of mutants are separated by other restriction fragments that carry for other genes (see Fig. 17). Based on complementation tests (49), these mutants in cluster IV represent at least three genes (genes 3, 16, and 20; see Fig. 17). Therefore, the nine mutants probably represent at least four genes (the fourth being gene 21), some of which could code for baseplate components, but only one of which could code for the tube, as it is probably (by analogy with other phages) composed of only one polypeptide species.

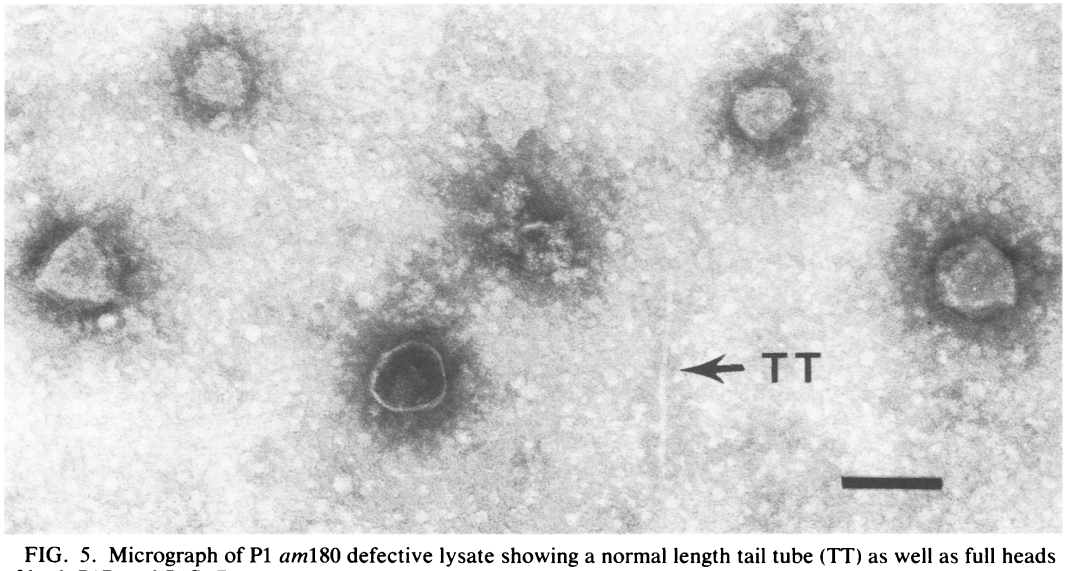

FIG. 5. Micrograph of P1 *am*180 defective lysate showing a normal length tail tube (TT) as well as full heads of both P1B and P1S. Bar, 100 nm.

Mutant 180 (in cluster V; Fig. 5) shows complete heads and tail tubes without sheaths. Therefore, the defect of *am*180 is probably in sheath subunit production. No baseplates were seen attached to the tubes. This is probably due to the baseplates detaching from the completed tubes because, in amber$^+$ P1 lysates, contracted tails without baseplates are often seen (47). Alternatively, because *am*45, which has a defect in either the baseplate or the tube, does not complement *am*180, it may be that *am*180 is polar on *am*45 and is therefore missing both sheaths and baseplates.

Mutants 19 and 138 (both in cistron 5 in cluster VI) show particles which are complete except that all of the tails are semicontracted or contracted (Fig. 6). The defect of these mutants is probably in a baseplate component that is necessary for baseplate stability. That is, either this component is of minor importance for baseplate assembly or the mutation occurs at a location in the gene that allows formation of an almost complete polypeptide that does not prevent baseplate assembly. In either case, tail assembly and head-tail joining could occur, but the resultant baseplate would be unstable and cause tail contraction. Mutants with mutations in gene 9 in T4, which have a defect in baseplate completion (25, 27), show a phenotype similar (12) to that of these P1 mutants. Because the phenotype of these P1 mutants is different from that of the nine mutants (in clusters IV and V) discussed above, they could be defective in a different baseplate component and represent a different gene. This is supported by the fact that they are in a different linkage cluster and are physically separated by other P1 genome restriction fragments that carry other genes (see Fig. 17).

Mutant 79 in cluster VI produces polysheath and complete heads attached to short tails. These tails have sheaths of various lengths (Fig. 7) with baseplates and tail fibers attached, and it is apparent that the defect of *am*79 affects tail length. In some instances the tails are so short that although a baseplate is seen, it cannot be determined whether any sheath subunits are present.

Mutants 26, 32, and 109 in cluster VI produce complete heads, polysheath, and unit-length sheaths (Fig. 8). These sheaths (seen only in lysates of these mutants and mutants 27, 39, 53, 22, and 116; next paragraph) are similar in length to the sheaths on contracted tails, but they have no tail tube or baseplate. These structures indicate that baseplates and tubes were formed but subsequently slipped off the sheath. Such a phenotype suggests either that an unstable baseplate was formed and that the defect of these mutants is in a baseplate component or that there is a defect at the top of the tail similar to one of the defects described for the following mutants.

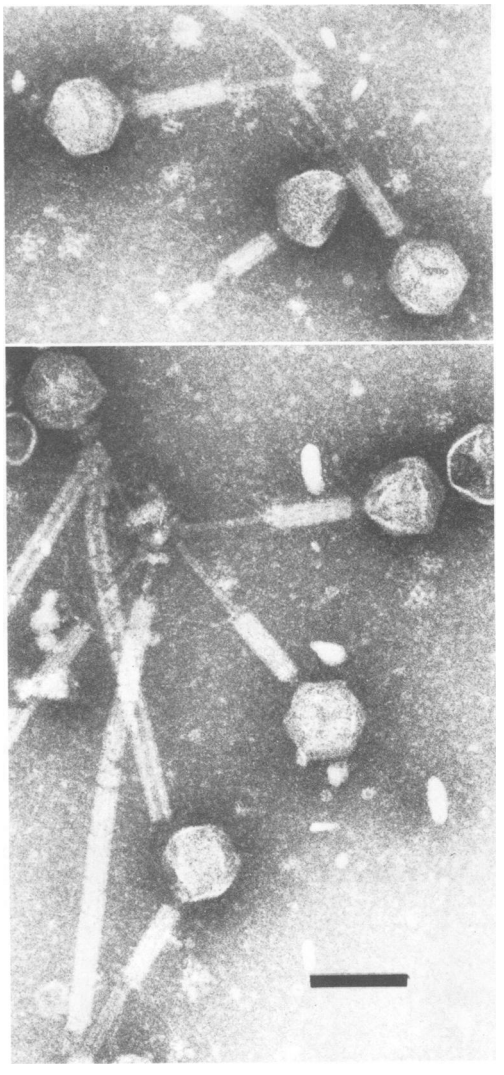

FIG. 6. Micrograph of P1 *am*19 defective lysate showing particles with tails that always have contracted sheaths. Bar, 100 nm.

Mutants 27, 39, 53, 22, and 116 (in cluster VI) produce complete heads, some polysheath, and unattached tails that have baseplates, tail fibers, and normal-length tubes (Fig. 9). However, the sheath on the tubes is contracted and has slipped down from the top of the tubes, and in some cases some of the sheath material is lost. In addition, unit-length sheaths are also seen, which could arise from the sheaths slipping completely off the tubes. This phenotype suggests that the defect of these mutants is in tail stability. Mutants 30 and 113 (which are in the

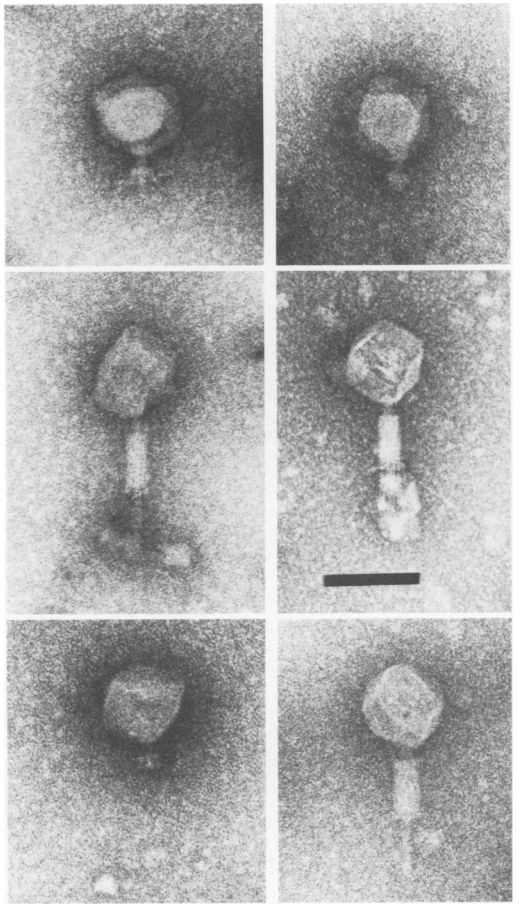

FIG. 7. Micrographs of P1 *am*79 defective lysate showing particles with shorter than normal length tails. Bar, 100 nm.

same cistron in cluster VII) have a similar phenotype (although no unit-length sheaths were seen), suggesting that their defect is in tail stability also. However, in addition to complete heads, polysheath, and tails with slipped sheaths, these mutants also produce contracted tails with polysheath attached (Fig. 10). These two groups of mutations (27, 39, 53, 22, and 116, and 30 and 113) are located in two different linkage clusters (Fig. 2); therefore, they are probably in two different genes. In T4, two genes (3 and 15) are required for tail stability. The gene 3 product is added to the top of the tube, where it acts as the terminator for sheath polymerization. The gene 15 product then forms a stable bond between the tube top and the top of the sheath and, at the same time, creates the head attachment site (25, 29). The two (or three, if mutations 26, 32, and 109 are included) groups of P1 mutations affecting tail stability may represent genes with functions similar to those of T4 genes 3 and 15. For example, the P1 genes could code for (i) the tail cap structure occasionally seen on P1 tails unattached to heads and (ii) the ringlike structure (seen attached to the base of the neck on tails where abnormal contraction has left the proximal part of the tube exposed; Fig. 9, inset), which is thought to stabilize the extended sheath and anchor it to the tail tube (47). In this regard, the contracted tails with polysheath attached seen in the cluster VII mutants could arise if the tail cap was missing and sheath subunits continued to polymerize onto the tail, past the top of the tube.

Tail tubes separate from sheaths are seen in lysates of some of the mutants in linkage cluster VI, where the tails are not attached to the heads (Table 1; Fig. 9 and 11). However, since they tend to occur in aggregates, they are not distributed evenly on the grid; thus, their presence may be overlooked in lysates of other mutants. This might explain why none were seen in *am*32 and *am*53 lysates. However, with these mutants, unit-length sheaths with or without tail tubes were seen, which confirms that tubes are made. Therefore, the absence of tail tube aggregates does not change our conclusions concerning the defects of these mutants. Additional structures seen in lysates of some of the mutants in cluster VI are stacked tails (Table 1; Fig. 6 and 9). These were seen infrequently, and their significance is unknown.

Mutant 142 (in cluster VIII) produces complete particles with semicontracted or contracted tails (similar to those seen with *am*19 and *am*138), complete heads, and polysheath. Therefore, the defect of *am*142 is probably in baseplate formation. Other mutants in cluster VIII (*am*139, *am*140, and *am*71) only produce complete heads and polysheath. Their defect could therefore be in baseplate or tube formation. It is not known how many cistrons these four mutants represent. If they are all in the same cistron, their defect could be in baseplate formation with *am*142 located in the distal part of this cistron.

Mutations affecting head assembly. Mutations affecting head assembly are located in linkage clusters II, V, IX, and X-1. Mutants in cluster II (150, 62, and 108; Fig. 12) and cluster X-1 (16, 64, 136, 131, 43, and 112; Fig. 13) produce complete tails and unattached empty heads in head/tail ratios of 1:1 to 1:3. (A total of 245 to 873 particles were counted per mutant, using electron micrographs of randomly selected fields from several preparations.)

In complementation tests (49), *am*150 and *am*62 give negative results. Because of this and because the phenotypes of the two mutants are similar, the mutations that they represent are

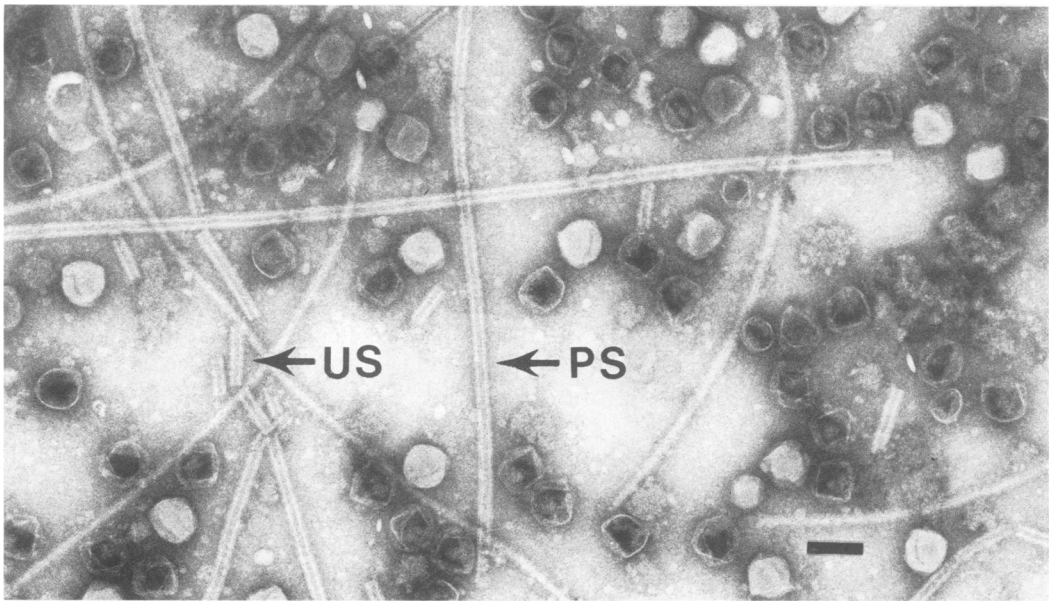

FIG. 8. Micrograph of P1 *am*26 defective lysate. In addition to normal full heads, there are polysheath (PS) and unit-length sheaths (US) or fragments thereof. The long curved structures are bacterial flagella. Bar, 100 nm.

probably in the same gene, which we will refer to as gene 4, a designation originally made by Scott (39) for *am*7. (Complementation results with *am*62 and *am*108 were ambiguous; therefore, we are unsure whether the mutation in *am*108 is located in this gene.) For similar reasons and because the mutants in linkage cluster X-1 are rescued from two adjacent fragments of the P1 genome (see Fig. 17), one of which also contains at least part of the P1 *c*1 gene and the other of which is flanked by a 0.62-kilobase-pair (kb) fragment which contains at least part of gene 10, the mutations in linkage cluster X-1 are assigned to a single gene (gene 9, a designation originally made by Scott [39] for *am*16), although there is a possibility that these mutants could represent more than one gene.

The empty heads produced by gene 9 and cluster II mutants are similar (in size and in the thickness of the capsid shell) to empty mature heads seen in amber$^+$ lysates. Therefore, they are presumed to be mature heads that are lacking DNA, rather than proheads.

In T4, mature, empty, unattached heads (and complete tails) are produced by mutants with defects either in various head completion genes (8, 11, 26) or in gene 49. Head completion genes are involved in neck assembly (gene 13), DNA packaging (genes 16 and 17), or unknown functions (genes 4 and 65). Gene 49 codes for DNase and is required for DNA packaging (14, 33). Heads of mutants in these genes are empty, either because they were not filled with DNA or because they were unstably filled and subsequently lost their DNA (8, 17). Genes in other phages that are involved in head completion are genes 4, 10, and 26 in P22 (6, 36), which code for three minor structural proteins required for head stability, and gene D in λ (24), which codes for a protein that is added to the mature capsid shell and whose presence is also required for DNA cutting (4, 23).

From their phenotype, the P1 gene 9 mutants could be defective in one of these functions. In this regard, Sternberg (personal communication) recently found that, unlike mutants in genes 4, 8, and 23, gene 9 mutants cannot cleave P1 DNA at *pac*, the site for initiation of DNA packaging (see Fig. 17); therefore, like genes 2 and 3 in phage P22 (31), the P1 gene 9 product is involved in the recognition and cleavage of P1 DNA at *pac*. With other phages, conversion of proheads to mature heads usually occurs concomitantly with DNA packaging. Gene 9 mutants apparently cannot initiate DNA packaging. Therefore, in P1 either conversion of proheads to mature heads can occur independently of DNA packaging or P1 proheads resemble mature heads in size and shell thickness.

The cluster II mutants could also be defective in one of these functions (except for DNA cleavage because, as mentioned above, Sternberg found that cluster II mutants can cleave P1 DNA at the *pac* site).

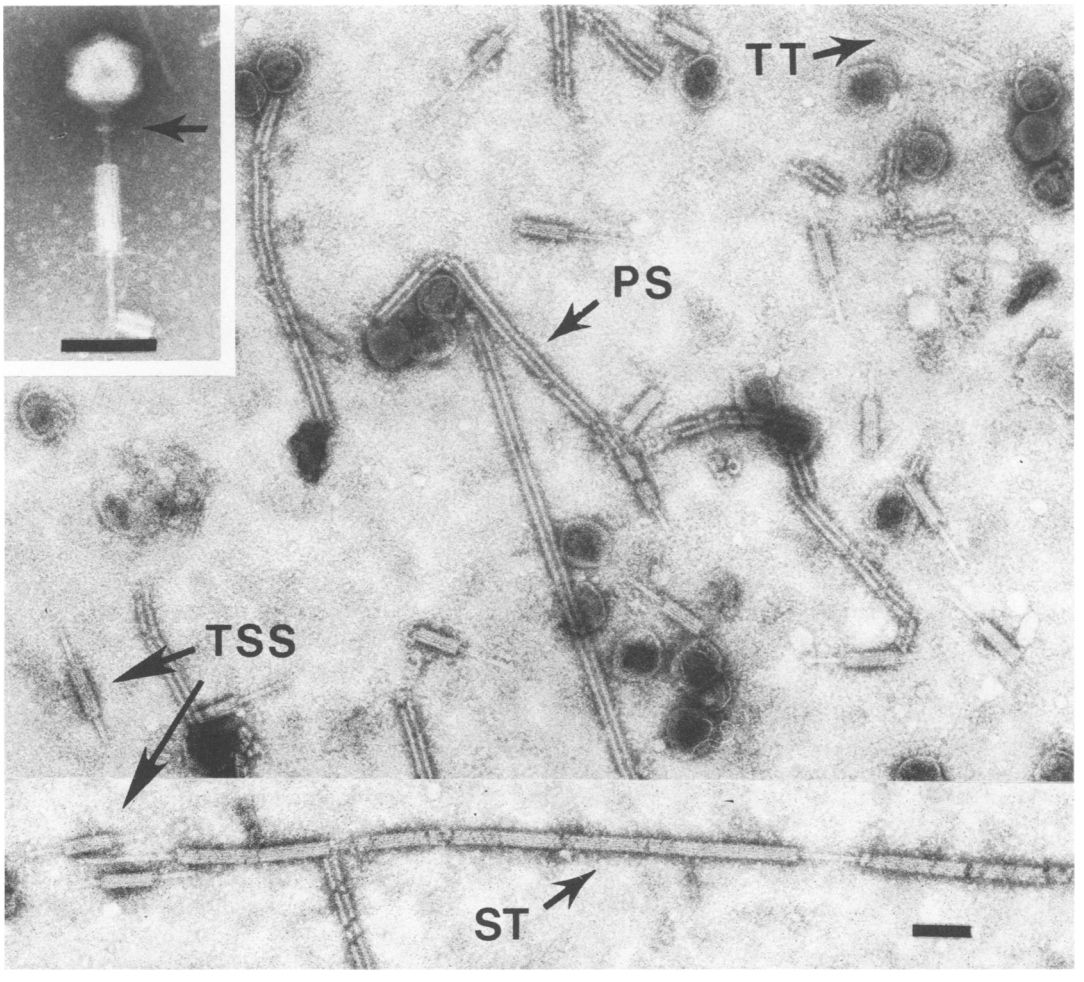

FIG. 9. Micrograph of P1 *am*27 defective lysate showing several kinds of tail structures. Note the tail tube aggregate (TT), polysheath (PS), tails with slipped sheaths (TSS), and stacked tails (ST). Inset shows an amber$^+$ P1 particle from a CsCl gradient; after prolonged exposure to CsCl, there is abnormal tail contraction, i.e., the tail sheath has contracted and slid down the tube, but a ringlike structure with or without some sheath subunits remains at the junction between the proximal end of the tube and the neck (see text). Bar, 100 nm.

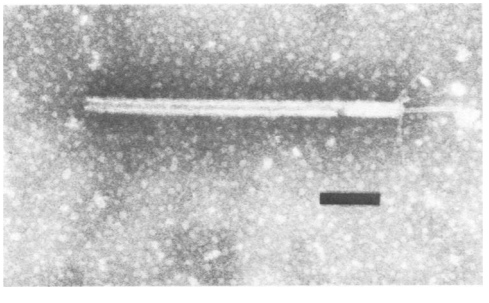

FIG. 10. Micrograph of P1 *am*30 defective lysate. Polysheath appears to be attached to the proximal end of this characteristically contracted tail, which otherwise appears to be normal in having both a baseplate and tail fibers. Bar, 100 nm.

Like the mutants in linkage clusters II and X-1, a single mutant (*am*115) in cluster V and the mutant (*am*13) that represents cluster IX (i.e., gene 8) produce complete tails and unattached empty heads. With *am*13, the head/tail ratio is 1:2 (1,967 particles were counted). However, with *am*115, very few heads were seen (the head/tail ratio was 1:30, with 431 particles counted), and input phage could account for these heads. Attached to the tails of both *am*115 and *am*13 mutants are structures resembling the neck and head-neck connector (Fig. 14). The neck and head-neck connector are part of the head. This suggests that the heads were originally assembled, filled with DNA, and attached to the tails, but were unstable and subsequently either disintegrated (*am*115) or dissociated from

FIG. 11. Micrograph of P1 *am*116 defective lysate showing aggregates of tail tubes. No single tube is longer than normal length. Bar, 100 nm.

the tail, leaving behind at least some of the neck and head-neck connector (*am*13). Such instability could be due to the absence of a minor head protein, e.g., a minor head shell protein (*am*115) or a head-neck connector protein (*am*13). Alternatively, because so few heads are seen in *am*115 lysates, *am*115 could be defective in the major head protein. In this case, the structures seen would not be a neck and head-neck connector but an aberrant structure similar to that seen in T4 (called the extension [8]), which consists of an aberrant accumulation on the top of the tail of five proteins normally assembled into the head as part of the neck and head-neck connector or added to the head-neck connector after head-tail joining.

Mutations affecting particle maturation. Mutations affecting particle maturation (47, 141, 34, 128, 132, and 57) comprise linkage cluster I. The mutants in cluster I do not show complementation (49) and are rescued from a 0.92-kb restriction fragment of the P1 genome flanked by fragments carrying other genes (see Fig. 17); therefore, these six mutations are probably in the same gene (gene 1). Particles produced by the six mutants are complete except that, in all of the mutants except 57, heads tend to be empty and the tails are in various stages of contraction (Fig. 15). Mutant 57 produces complete particles with at least partially filled heads and extended sheaths (Fig. 16). These phenotypes suggest that the defective polypeptide allows assembly of the

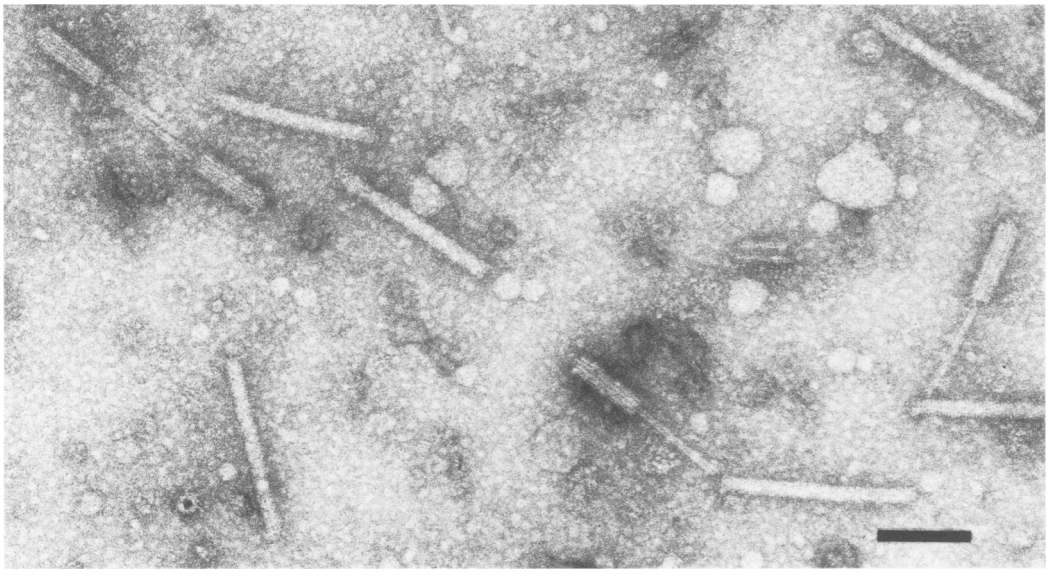

FIG. 12. Micrograph of P1 *am*108 defective lysate. The tails appear to be normal; heads, not seen here, are also produced. Bar, 100 nm.

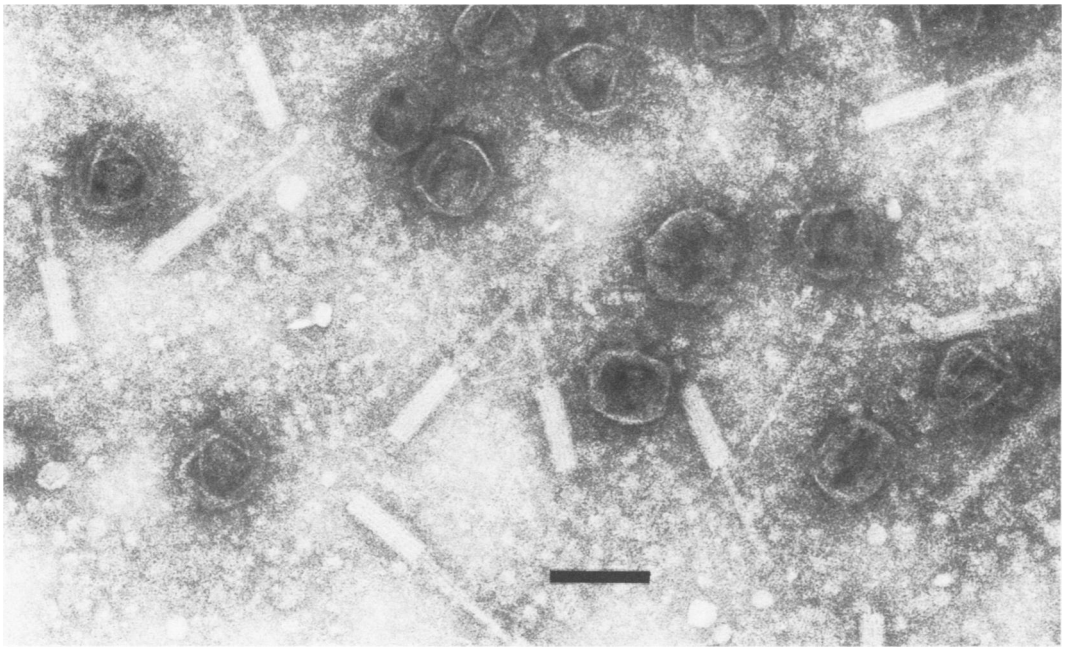

FIG. 13. Micrograph of P1 *am*64 defective lysate. The heads are the same size as mature heads, but they are always empty; the tails are normal, their contraction being an artifact of preparation procedures. Bar, 100 nm.

complete particles but that these particles are either morphologically complete but noninfective (*am*57) or unstable. Morphologically normal particles are produced by other phages, e.g., P22 mutants defective in genes 7, 16, and 20 (6, 36) and T4 mutants (11, 12, 26) defective in genes 2, 4, 11, 12, 50, 64, and 65 (which produce at least some morphologically normal phages). Genes 11 and 12 are tail genes, coding for a baseplate component and short tail fibers, respectively. All of the remaining gene products are incorporated into the head at early stages of assembly, but their functions vary; e.g., some are involved in the DNA injection process, and some (in T4) are involved in cleavage of head proteins. The P1 mutants could have one of these head gene defects (although it is not known whether there is cleavage of P1 head proteins). Alternatively, because of the instability of the tail, they could have a defect in a tail gene, e.g., a baseplate gene. The difference observed between *am*57 and the other mutants in this cluster could be explained by the *am*57 mutation being in the distal part of the gene to give a more complete polypeptide and hence a more stable particle. In support of this is the fact that *am*57 is located at one end of the cluster with respect to the other five mutants examined (Fig. 2).

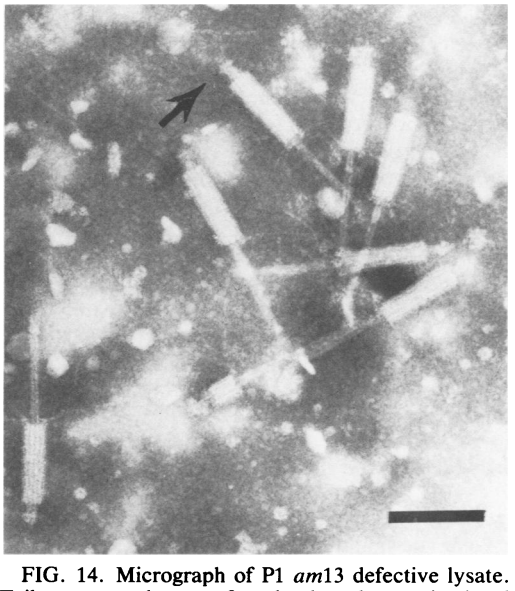

FIG. 14. Micrograph of P1 *am*13 defective lysate. Tails are normal except for a knob at the proximal end (arrow). Bar, 100 nm.

Mutations affecting host cell lysis. Cells infected separately with eight mutants that cannot cause cell lysis (gene 17, linkage cluster III, or gene 10, cluster X-2) or that cause premature cell lysis (gene 2, cluster IV) were examined by electron microscopy at the incubation time (110 min) at which lysis would be complete in cells infected with lysis-positive mutants.

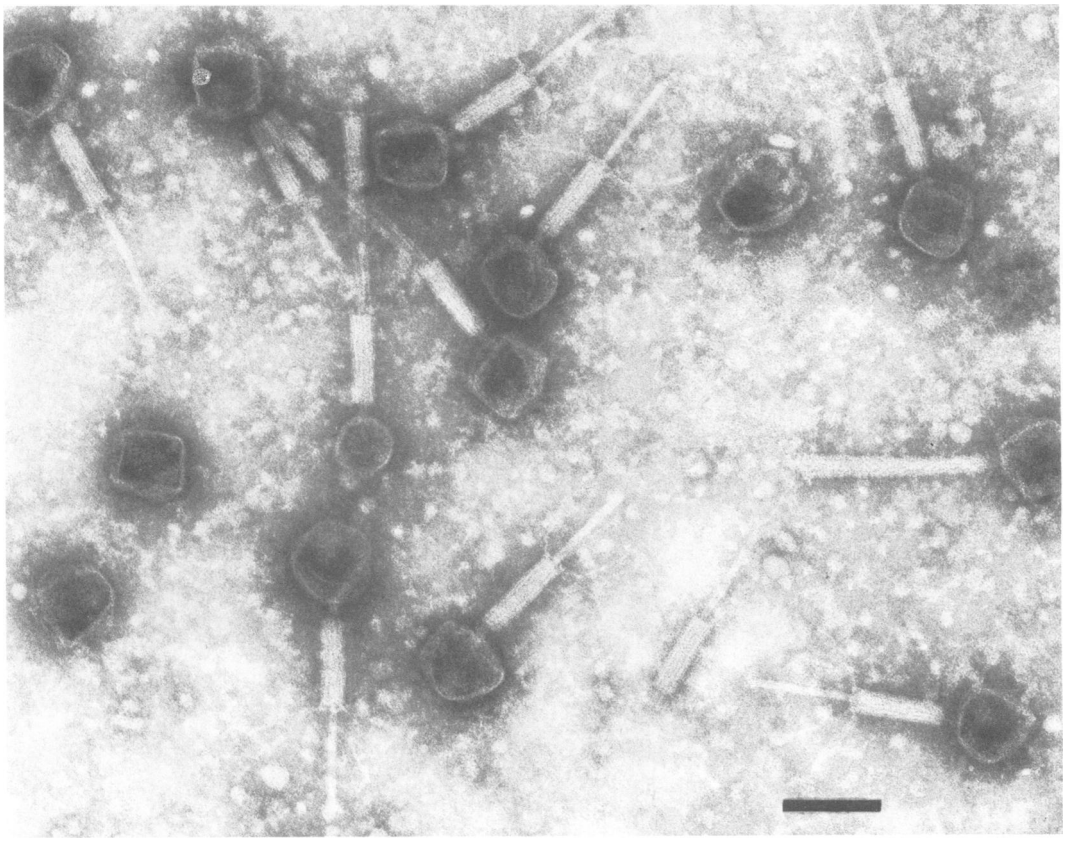

FIG. 15. Micrograph of P1 *am*47 defective lysate. Particles appear to be normal except for empty heads (mature size); normal tails are in various stages of contraction. Bar, 100 nm.

Mutants (23, 144, 73, and 134) having mutations in gene 17 showed intact cells as expected and, occasionally, some cells that had lost some of their contents but were full of phage particles. Very rarely, some complete phage, which could have been input phage, were seen outside the cells. These results are consistent with the findings (50) that artificially lysed cells infected with these mutants produce viable phage particles and give positive results in serum blocking assays and that phage particles are seen in thin sections of unlysed cells infected with *am*144 (or *am*20, which has a mutation in the same gene) and support the conclusion that these mutants are defective in a lysis function.

Mutants (178 and 105) having mutations in gene 10 showed intact cells and, very rarely, some complete phage, which were probably input phage. These mutants did not show serum blocking power, even after sonication to disrupt the unlysed cells and to release any tail fiber antigen that might be present. These results are consistent with the findings (50) that artificially lysed cells infected with these mutants do not produce viable phage particles and that no phage particles are seen in thin sections of unlysed, infected cells. Therefore, the results are consistent with the conclusion (50) that gene 10 mutants cannot synthesize late proteins (including the lysis proteins) and that gene 10 may code for a regulator of late gene expression for P1.

Mutants (31 and 56) having mutations in gene 2 showed very few particles, and these were complete (except that the presence of tail fibers could not be determined). These mutants cause premature lysis and may have a defect in a lysis regulator (50). In addition to very few particles being seen by electron microscopy, serum blocking assays are negative with these mutants, and the burst size is low (50). These results can all be explained by too few phage particles being produced by the time that lysis occurs.

DISCUSSION

Gene designations of mutations affecting P1 morphogenesis. We determined the phenotypes of 47 P1 amber mutants by use of electron microscopy and serum blocking assays. Eleven

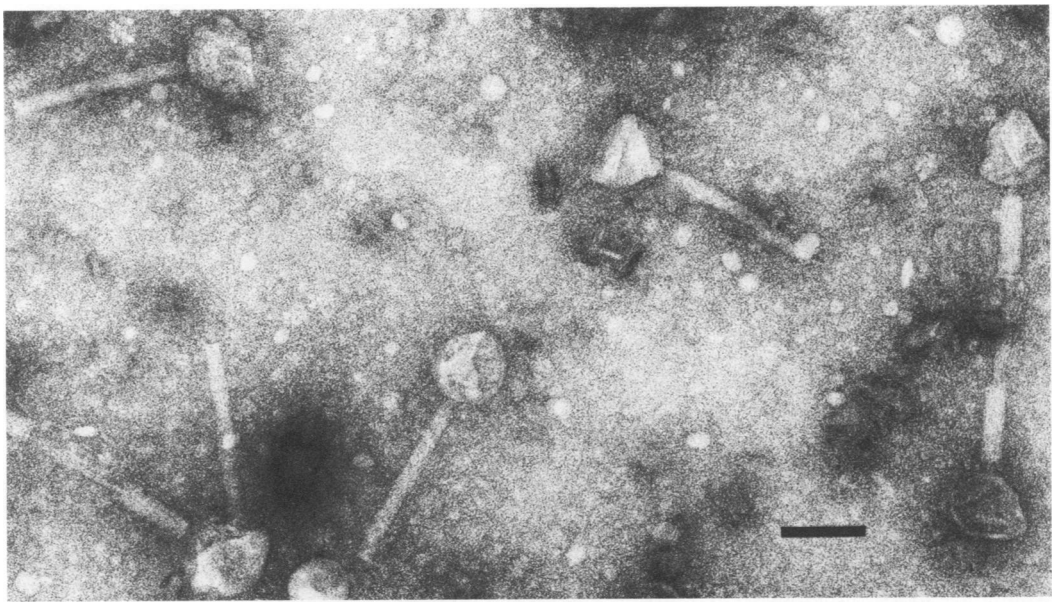

FIG. 16. Micrograph of P1 *am*57 defective lysate. Particles appear normal; irregular outline of heads may possibly be due to flattening as a consequence of being only partially filled with DNA. Bar, 100 nm.

mutants (Fig. 17) showed head defects, thirty showed tail defects, and six had a defect in particle maturation that could be either in the head or in the tail. When we consider the unambiguous results from complementation tests, the genetic and physical positions of the mutations, and the phenotypes of the mutants, we can assign most of these mutations to genes (Table 1 and Fig. 17). Exceptions are mutations 108, 33, 66, 74, and 142, which could be located in different genes than those indicated (i.e., genes 4, 19, 20, and 26). *am*108 gives ambiguous complementation test results with other gene 4 mutants and thus may be in a different gene. Results of serum blocking assays did not distinguish between the possibilities that mutants 33, 72, and 66 could be in the same gene (gene 19) or in different genes. Although mutations 139, 140, and 71 (in cluster VII; gene 26) result in a slightly different phenotype than that of *am*142 (Table 1), these four mutations could be in the same gene because they are located in a relatively short region of the genome (Fig. 17). However, it is not known whether mutations 74 and 49 are in the same gene (gene 20) because, although they show similar phenotypes, they give ambiguous results in complementation tests (49), and the precise location of *am*74 on the physical map is unknown.

Mutations affecting head morphogenesis. As a result of these gene designations, it is seen that the 11 mutations causing head defects are located in four (or at most six) genes (genes 4, 23, 8, 9, and perhaps the particle maturation gene 1 and a gene represented by *am*108). In T4, head assembly involves the products of at least 20 genes, about half of which constitute the finished particle (53). P22 head assembly requires the products of 11 genes, about 6 of which are in the finished particle (53). With its head shell, head-neck connector, and neck structures, P1 heads are at least as complex as P22 heads. In support of this, results from gel electrophoresis examination of P1 particles indicate that they consist of 28 proteins, of which 15 are in the head, 9 are in the tail, and 4 are either in the head or the tail (51). Of the 15 (to 19) head proteins, 4 are coded by a region of the genome, between map units 24 to about 32, that is not essential for particle formation. However, it is not known whether any of the remaining 11 to 15 head proteins result from cleavage or fusion of polypeptides during head assembly. In addition, it is not known whether there are any proteins (such as the scaffolding protein in P22) that are not components of the final virion structure. Nevertheless, it is likely that more than four (to six) genes are required for P1 head assembly. In this regard it is of interest to note that adjacent to head genes 4 and 8 (Fig. 17), there are regions of the genome for which no functions are known and which might carry further head genes. Razza et al. (38) have described temperature-sensitive mutants in two new genes (genes 13

and 14) that are located near gene 4 and that are required for lytic growth of P1. These could be head genes. (Another new gene described by Razza et al., gene 15, is located near genes 22 and 23 and could be either a head or a tail gene.)

Only three phenotypes are produced by amber mutations in the four head genes. These phenotypes are (i) complete tails and separate empty heads (genes 4 and 9), (ii) complete tails with necks and head-neck connectors and separate empty heads (gene 8), and (iii) complete tails with necks and head-neck connectors (or extensions) (gene 23). As mentioned above, gene 9 mutants are defective in a function required for DNA cleavage at *pac* (N. Sternberg, personal communication). The defect of cluster II mutants is unclear, but could be in a minor protein (such as a neck protein) or in a protein required for DNA packaging (other than that required for DNA cleavage at *pac*). The second and third phenotypes suggest either a defect in a minor head protein that leads to a filled, attached, but unstable head or a defect in the major head protein that leads to an accumulation of the neck and head-neck connector proteins at the top of the tail to form a structure called the extension by Coombs and Eiserling (8). Head-defective phenotypes not seen, which might represent head genes not as yet detected, are as follows. (i) Proheads. Unless P1 proheads resemble mature heads, none were seen. Other phages produce proheads in defective lysates of mutants having mutations representing various different genes. Therefore we would expect to have more than one gene in which the mutant allele results in prohead production. In this regard, it could be, as mentioned above, that P1 proheads are unstable and can convert to mature heads independently of DNA packaging. (ii) No heads. In other phages, mutations in the major head gene result in mutants that do not produce heads. Although P1 mutants that do not produce any heads at all have not been found, the gene 23 mutant produces very few heads (1 head per 30 tails), so this gene might code for the major P1 head protein. (iii) Spiral head structures, such as those seen in mutants of P22 defective in scaffolding protein (28) or in mutants of λ defective either in the minor head proteins B and C (24) or in the scaffolding protein Nu3 (37). (iv) Polyheads, such as those seen in T4 mutants defective either in the core protein, an internal protein, the vertex protein, or in proteins required for correct capsid initiation (12, 13, 30, 40, 56). Polyheads are also seen in λ mutants defective in genes B and C. (v) Particles with only small heads (P1S particles). A unique property of P1 is that, in addition to normal, infectious, big-headed (P1B) particles, it also produces 10 to 20% noninfectious, small-headed P1S particles (47). It would be useful in studying head size determination to have a mutant that produces P1S particles only. So far, the only P1 phage that produce an increased proportion of P1S particles (i.e., 50% P1S and 50% P1B particles) are those that are deleted for a region of the genome that is not essential for particle morphogenesis (i.e., map units 24 to 32) (Fig. 17) (20). The determinant in this region for this change in the P1S/P1B ratio is designated *vad* for viral architecture determination (20).

Mutations affecting tail morphogenesis. The 30 mutations causing P1 tail defects are located in at least 12 genes (genes 19, 20, 16, 3, 21, 22, 5, 6, 24, 7, 25, and 26; Fig. 17). There could be up to five additional tail genes (represented by mutants 72, 66, 49, and 142 and perhaps including gene 1, which is involved in particle maturation). In T4, tail assembly (including tail fibers) requires the products of 29 genes, and all but 7 of them become part of the final structure. The P1 tail is less complex than that of T4 (i.e., the baseplate is thinner and less well defined). Results from gel electrophoresis studies indicate that the P1 tail is composed of between 9 and 13 proteins (51). However, it may be that some of the baseplate components are small and required in low quantities and so were not resolved by gel electrophoresis.

Of the structural tail genes in T4, 1 gene codes for the tube; 1 for the sheath; 4 for the tail fibers; 14 for the baseplate; and 2 for the structures that add to the top of the tail to stabilize it. The 12 to 17 P1 tail genes consist of 1 (gene 22) coding for the sheath; between 6 (genes 20, 3, 16, 21, 5, and 26) and 10 (the additional genes being gene 1, gene 24, and genes represented by *am*49 and *am*142) coding for baseplate or tube production (of which only 1 would code for tube production); 2 or 3 (genes 7, 24, and 25) coding for tail stabilization; 1 (gene 6) affecting tail length; and 1 (gene 19, represented by *am*72) or more (represented by *am*33 and *am*66) coding for tail fibers. In addition, Razza et al. (38) found two genes (genes 11 and 12, represented by temperature-sensitive mutants) that are located in the vicinity of gene 19 and may code for tail fiber structural proteins. In summary, we may not know for all of the tail genes which code for structural proteins and which code for nonstructural proteins, but mutations affecting each of the tail components visible by electron microscopy are represented (with a possible exception of the tail tube).

Gene 19 mutants do not have tail fibers and do not show serum blocking power (for this discussion we shall assume that mutations 33, 72, and 66 are all in gene 19, although this may not be so). Therefore, gene 19 is a structural gene that probably codes for the distal part of the tail

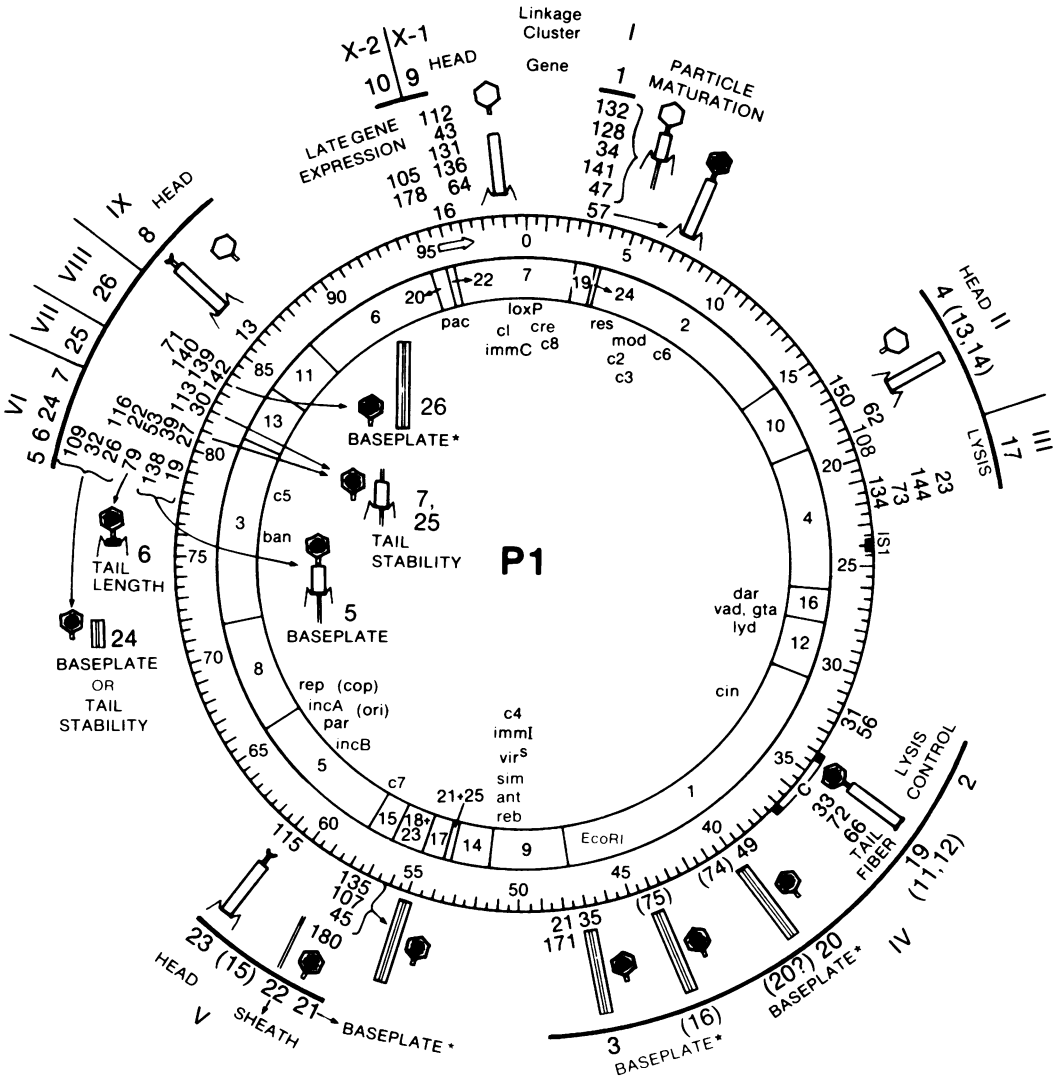

FIG. 17. Map of the bacteriophage P1 genome, modified from that of Yarmolinsky (57). The inner circle represents the physical genome, divided into the numbered digestion fragments generated by restriction endonuclease *Eco*RI (2). Genetic symbols within this circle represent functions not required for phage morphogenesis (except *pac*); for a complete list of these functions and their references, see Yarmolinsky (57). *pac* is the site where DNA packaging initiates (arrow indicates direction of packaging). Other symbols and functions: *c* genes, establishment and maintenance of lysogeny (*c*6 and *c*8 were found in phage P7); *imm*C and *imm*I, bipartite immunity system; *res* and *mod*, restriction and modification; *dar*, defense against restriction; *vad*, viral architecture determination; *gta*, generalized transduction affected; *lyd*, lysis delay; *cin*, C loop inversion; *vir*^{s}, virulence; *sim*, superimmunity; *ant* or *reb*, antagonism or bypass of *c*1 repressor; *par*, plasmid partition; *inc*A and *inc*B, plasmid incompatability; *rep*, plasmid replication; *ori*, origin of replication; *cop*, plasmid copy number; *ban*, *dnaB* analog; *lox*P, locus of crossover in plasmid; and *cre*, site-specific recombination. Outer circle, 100 map units (equivalent to percent of the 90-kb genome). On this circle, C denotes the invertible C loop; IS*1* denotes insertion sequence 1. Between the outer circle and the arcs are numbers representing amber mutations. The locations of these amber mutations on the physical map were determined by marker rescue experiments, using cloned fragments of P1 DNA (21, 34, 38, 43, 45). The arcs denote extent of linkage clusters (roman numerals). Numbers outside these arcs denote genes (gene numbers 5, 6, 24, 7, and 25 are repeated above their relevant functions). A query denotes the uncertain gene designation of *am*74. Diagrammatic representations of the amber mutant phenotypes and functions of the genes are noted. Asterisks beside baseplate notations mean that one of these genes could code for the tail tube. Imprecise locations of genes or amber mutations are denoted by parentheses around the relevant symbol or number. Genes 11 through 15 are represented by temperature-sensitive mutations only (not shown) and have not been phenotyped. Rescue tests and two-factor crosses have shown amber mutant 75 (gene 16) to be located between mutants 74 and 35 and not around map unit 55 as indicated previously.

fiber. Mutant 72 is missing a 105,000-molecular-weight (MW) protein that, unless it is a fusion product, is the product of gene 19 (unpublished data). Toussaint et al. (45) located the gene 19 mutations within or near the P1 C loop (an invertible DNA region) because (i) this is the only region of homology shared with phage Mu (i.e., the Mu G loop) and (ii) the amber$^+$ alleles of these P1 mutants are rescued from Mu. The P1 C loop is 3 kb long and flanked by two 0.62-kb inverted repeats. The 105,000-MW protein coded by gene 19 would require a coding length of 2.9 kb of DNA. Gene 19 probably does not extend more than halfway (1.5 kb) into the G loop (by analogy with Mu [46]); therefore, the remaining portion (1.4 kb) of the gene would include one of the 0.62-kb inverted repeats and extend at least 0.78 kb outside the inverted repeat. If the 105,000-MW protein is not a fusion product, even more of gene 19 could be located outside the C loop. This is because amber$^+$ alleles of two Mu genes, one of which (*U*) is wholly within the G loop and another of which (*S*) is partially within the G loop and partially in the α region (16), are rescued from P1 (45). This suggests that there is another gene in addition to gene 19 in the P1 C loop. Products of both the *U* and *S* genes are required for Mu adsorption (46); therefore, in P1 the two analogous genes could code for the distal (gene 19) and proximal parts of the P1 tail fiber.

The following findings support the suggestion that gene 19 is partially outside the C loop and that it includes one of the inverted repeats. The P1-related phage P7, which has a 0.2-kb deletion (or substitution) within the right inverted repeat (7), produces a 100,000-MW protein instead of the 105,000-MW P1 tail fiber protein (51). (These findings also suggest that gene 19 extends to the right rather than to the left of the C loop.) Transcription of gene 19 is leftward from *am*49 (because *am*49 is polar on gene 19; Fig. 2). Also, no polypeptide fragment of the 105,000-MW protein is seen after sodium dodecyl sulfate-polyacrylamide gel electrophoresis of *am*72 (unpublished data). Therefore, unless the amber fragment has been degraded, this mutation must be near the end of gene 19 that is proximal to where transcription is initiated.

The model of gene 19 as being partially within and partially outside the C loop is consistent with the following findings: (i) Mu and P1 have partial serological cross-reactivity (45), and (ii) the host range specificities of these two phages are within (or near) these invertible regions (45, 46). By analogy with T4 (3), these host range specificities are probably located in the tail fiber genes of the phages.

Assembly of P1 particles. By examining the structures obtained in defective lysates, it is seen that P1 heads and tails can be assembled independently. This suggests that, like T4, these P1 structures have independent assembly pathways. However, in P1, tail fibers are often seen attached to headless tails. Therefore, unlike T4 tail fibers, P1 tail fibers can attach to the tail before head-tail joining occurs. (This had already been suspected because the P1 tail fibers are not long enough to reach from the baseplate to the head, such a length being required for the addition of tail fibers to T4 particles.)

Distribution of mutations. The P1 amber mutations affecting particle morphogenesis are not equally distributed among the designated genes. For example, including mutations not studied in the work reported here (Fig. 2), there are 13 mutations in gene 1 and only 1 mutation in each of genes 22, 23, and 8. We do not know the sizes of these genes, but it may be that there are "hot spots" of mutation (obtained by hydroxylamine), as was found in P22 (36). In support of this, we do know that there are 10 mutations in gene 10, which codes for a protein of 64,000 MW (18) involved in late gene expression (50), and a maximum of 3 mutations in gene 19, which codes for a 105,000-MW tail fiber protein. The existence of hot spots of mutation could explain why some of the head-defective phenotypes described above have not yet been seen.

Correlation of phenotypes with the P1 genetic and physical maps. The 103 P1 amber mutations have been assigned (49) to 10 linear arrays or linkage clusters (I through X; Fig. 2). Because complementation tests in liquid often gave ambiguous results and not all mutants were tested in all combinations, only some of the mutations were put into groups that showed no complementation. The 55 amber mutant phenotypes (i.e., including mutations in genes 17, 2, and 10) that we determined correlate with the linear arrays of the corresponding mutations. For example, in linkage cluster VI, mutants 26, 32, and 109 show one phenotype and mutants 27, 39, 53, 22, and 116 show another. In addition, except for mutants 180 and 45 (which may be polar mutants), all mutants tested that were found not to complement (Fig. 2) showed the same phenotype.

We previously suggested (49) that the phenomenon of linkage clusters might result from a variety of underlying causes, such as recombination hot spots, long segments of silent DNA, or regions for which there were no known mutations. The physical position of the mutations comprising the linkage clusters is now known (Fig. 17) (57), and it can be seen that the clusters consist of single genes or groups of genes and that the demarcations between some of these linkage clusters (i.e., II/III, VI/VII, VII/VIII, VIII/IX, and X-2/X-1) are due to recombination

between these genes or gene groups. The reason why some linkage clusters are comprised of single genes and some are comprised of gene groups is unknown, unless hot spots of recombination are invoked. Other demarcations between linkage clusters, such as I/II, III/IV, IV/V, V/VI, and IX/X-2, are due to long segments of DNA that either contain other genes (e.g., coding for immunity) or for which no mutations are known, or a combination of these two reasons. (It may be that there are no long segments of silent DNA because, for example, some morphogenetic genes [especially head genes] are still undetected.) Between linkage clusters X-1 and I (i.e., at the ends of the vegetative map), there is a shorter segment of DNA that codes for part of the P1 immunity system. However, this region has also been shown to contain a recombination hot spot (*loxP* [44]), which alone could account for the demarcation between these two clusters.

Clustering of functionally related genes. The physical and genetic maps of P1 show considerable clustering of genes having related functions. Such clustering could be advantageous for regulating the assembly of substructures, such as, for example, baseplates. We do not know whether gene 1 is a head or a tail gene. Excluding gene 1, the known tail genes are located in three regions. The approximate physical positions of these regions are map units 34 to 49, 56 to 59, and 78 to 84.5. Within these regions, some similar functions are located together. In the first region there are three to five tail fiber genes and three to four baseplate (or tail tube) genes. In the second region we found one tail sheath gene and one baseplate (or tail tube) gene. It may be, by analogy with T4 (54), that the single P1 tail tube gene is located in this region beside the sheath gene. In the third region we found one or two baseplate genes, a tail length gene, two or three tail stability genes, and one or two baseplate or tail tube genes. In this region the baseplate genes are separated by other tail genes. However, unlike genes 3 and 15 of T4 (54), the two to three P1 tail stability genes are located together.

The four to five known P1 head genes are in four regions of the genome. This would argue against clustering of functionally related head genes. However, some expected P1 head genes have not yet been detected and could be located in two main regions for which there are few known genes. One of these regions comprises map units 10 to 20 and could theoretically code for about 10 genes, including head gene 4, the head gene represented by *am*108 (if different from gene 4), and genes 13 and 14 found by Razza et al. (38). The other region comprises map units 84.5 to 94, which could code for 9 or 10 genes, including head gene 8. In addition, it is interesting to note that head gene 9, which is adjacent to *pac*, the site at which DNA packaging is initiated, has now been found to code for P1 DNA cleavage at this site (N. Sternberg, personal communication).

In addition to lysis gene 17, P1 probably has a second lysis gene (*lyd* [20]), analogous to the *S* gene of λ, located somewhere between map units 24 and about 32. Therefore, these two lysis genes and a lysis regulator gene (gene 2), although not all adjacent to each other, are located within a region spanning less than 15% of the P1 genome (map units 20 to about 33).

Gene 10, which regulates late gene expression (50), is located approximately between map units 94 and 96. Gene 10 is probably analogous to gene Q in λ, which is adjacent to genes (*O* and *P*) involved in DNA synthesis. If similar clustering occurs in P1, such DNA synthesis genes could be to the left of gene 10, in a region for which no genes have as yet been found.

We do not know the full extent of clustering in P1 because of the regions of the genome for which no genes are known. That is, the regions mentioned above (between genes 8 and 10 and genes 1 and 4) and another region approximately between map units 67 and 76.

In addition, very little is known about the transcription patterns in P1, so we do not know how much the clustering of functionally related genes is related to their cotranscription. (An exception is that *am*49 is polar on gene 19, and the gene it represents is therefore probably cotranscribed with gene 19.)

Genome organization of P1 compared with that of other phages. The functionally related genes of P1 are not clustered as conservatively as they are, for example, in λ, in which all head genes are in one region, adjacent to all of the tail genes in another region, and in which all the genes determining other functions (such as integration, excision, recombination, gene regulation, replication, and lysis) are in the remaining region of the genome (10). The organization of the P1 genome more closely resembles that of T4 (54), in which the tail genes are located in at least six regions and the head genes in at least five regions. In T4, these morphogenetic gene clusters are interspersed with genes concerned with, for example, DNA metabolism. In P1, morphogenetic gene clusters are interrupted by many genes that are expressed in the prophage, such as the genes for establishment and maintenance of lysogeny, plasmid replication, immunity, or restriction and modification of DNA. As for the precise functions of the genes for which we have amber mutants, further investigations with other techniques are required.

ACKNOWLEDGMENTS

We thank Jean Morningstar for her technical assistance, particularly with serum blocking power tests, Mark Urbanowski for his photographic assistance, and Michael Feiss for reading the manuscript. We thank Michael Yarmolinsky and Nat Sternberg for communicating unpublished data. We thank Mary Smithson for typing the manuscript.

This work as supported by grant PCM 78-23223 from the National Science Foundation.

LITERATURE CITED

1. **Arisaka, F., J. Tschopp, R. van Driel, and J. Engel.** 1979. Reassembly of the bacteriophage T4 tail from the core-baseplate and the monomeric sheath protein P18: a cooperative association process. J. Mol. Biol. **132**:369–386.
2. **Bächi, B., and W. Arber.** 1977. Physical mapping of *Bgl*II, *Bam*HI, *Eco*RI, *Hind*III and *Pst*I restriction fragments of bacteriophage P1 DNA. Mol. Gen. Genet. **153**:311–324.
3. **Beckendorf, S. K.** 1973. Structure of the distal half of the bacteriophage T4 tail fiber. J. Mol. Biol. **73**:37–53.
4. **Becker, A., and M. Gold.** 1975. Isolation of the bacteriophage lambda A-gene protein. Proc. Natl. Acad. Sci. U.S.A. **72**:581–585.
5. **Bertani, G.** 1951. Studies on lysogenesis. I. The mode of phage liberation by lysogenic *Escherichia coli*. J. Bacteriol. **62**:293–300.
6. **Botstein, D., C. H. Waddell, and J. King.** 1973. Mechanism of head assembly and DNA encapsulation in *Salmonella* phage P22. I. Genes, proteins, structures, and DNA maturation. J. Mol. Biol. **80**:669–695.
7. **Chow, L. T., T. R. Broker, R. Kahmann, and D. Kamp.** 1978. Comparison of the G DNA inversion in bacteriophages Mu, P1, and P7, p. 55–56. *In* D. Schlessinger (ed.), Microbiology—1978. American Society for Microbiology, Washington, D.C.
8. **Coombs, D. H., and F. A. Eiserling.** 1977. Studies on the structure, protein composition and assembly of the neck of bacteriophage T4. J. Mol. Biol. **116**:375–405.
9. **DeMars, R. I.** 1955. The production of phage-related materials when bacteriophage development is interrupted by proflavine. Virology **1**:83–99.
10. **Echols, H., and H. Murialdo.** 1978. Genetic map of bacteriophage lambda. Microbiol. Rev. **42**:577–591.
11. **Edgar, R. S., and I. Lielausis.** 1968. Some steps in the assembly of bacteriophage T4. J. Mol. Biol. **32**:263–276.
12. **Epstein, R. H., A. Bolle, C. M. Steinberg, E. Kellenberger, E. Boy de la Tour, R. Chevalley, R. S. Edgar, M. Susman, G. H. Denhardt, and A. Lielausis.** 1963. Physiological studies of conditional lethal mutants of bacteriophage T4D. Cold Spring Harbor Symp. Quant. Biol. **28**:375–394.
13. **Favre, R., E. Boy de la Tour, N. Segrè, and E. Kellenberger.** 1965. Studies on the morphopoiesis of the head of phage T-even. I. Morphological, immunological and genetic characterization of polyheads. J. Ultrastruct. Res. **13**:318–342.
14. **Frankel, F. R., M. L. Batcheler, and C. K. Clark.** 1971. The role of gene 49 in DNA replication and head morphogenesis in bacteriophage T4. J. Mol. Biol. **62**:439–463.
15. **Georgopoulos, C. P., R. W., Hendrix, A. D. Kaiser, and W. B. Wood.** 1972. Role of the host cell in bacteriophage morphogenesis. Nature (London) New Biol. **239**:38–41.
16. **Giphart-Gassler, M., R. H. A. Plasterk, and P. van de Putte.** 1982. G inversion in bacteriophage Mu: a novel way of gene splicing. Nature (London) **297**:339–342.
17. **Granboulan, P., J. Séchaud, and E. Kellenberger.** 1971. On the fragility of phage T4-related particles. Virology **46**:407–425.
18. **Heilmann, H., J. N. Reeve, and A. Puhler.** 1980. Identification of the repressor and repressor bypass (antirepressor) polypeptides of bacteriophage P1 synthesized in infected minicells. Mol. Gen. Genet. **178**:149–154.
19. **Howe, M. M., J. W. Schumm, and A. L. Taylor.** 1979. The S and U genes of bacteriophage Mu are located in the invertible G segment of Mu DNA. Virology **92**:108–124.
20. **Iida, S., and W. Arber.** 1977. Plaque forming specialized transducing phage P1: isolation of P1CmSmSu, a precursor of P1Cm. Mol. Gen. Genet. **153**:259–269.
21. **Iida, S., and W. Arber.** 1979. Multiple physical differences in the genome structure of functionally related bacteriophages P1 and P7. Mol. Gen. Genet. **153**:249–261.
22. **Israel, J. V., T. F. Anderson, and M. Levine.** 1967. *In vitro* morphogenesis of phage P22 from heads and base-plate parts. Proc. Natl. Acad. Sci. U.S.A. **57**:284–291.
23. **Kaiser, A. D., M. Syvanen, and T. Masuda.** 1975. DNA packaging steps in bacteriophage lambda head assembly. J. Mol. Biol. **91**:175–186.
24. **Kemp, C. L., A. F. Howatson, and L. Siminovitch.** 1968. Electron microscope studies of mutants of lambda bacteriophage. I. General description and quantitation of viral products. Virology **36**:490–502.
25. **Kikuchi, Y., and J. King.** 1975. Genetic control of bacteriophage T4 baseplate morphogenesis. III. Formation of the central plug and overall assembly pathway. J. Mol. Biol. **99**:695–716.
26. **King, J.** 1968. Assembly of the tail of bacteriophage T4. J. Mol. Biol. **32**:231–262.
27. **King, J.** 1971. Bacteriophage T4 tail assembly: four steps in core formation. J. Mol. Biol. **58**:693–709.
28. **King, J., E. V. Lenk, and D. Botstein.** 1973. Mechanism of head assembly and DNA encapsulation in *Salmonella* phage P22. J. Mol. Biol. **80**:697–731.
29. **King, J., and N. Mykolajewycz.** 1973. Bacteriophage T4 tail assembly: proteins of the sheath, core, and baseplate. J. Mol. Biol. **75**:339–358.
30. **Laemmli, U. K., E. Mölbert, M. Showe, and E. Kellenberger.** 1970. Form-determining function of the genes required for the assembly of the head of bacteriophage T4. J. Mol. Biol. **49**:99–113.
31. **Laski, F., and E. N. Jackson.** 1982. Maturation cleavage of bacteriophage P22 DNA in the absence of DNA packaging. J. Mol. Biol. **154**:565–579.
32. **Lindahl, G.** 1974. Characterization of conditional lethal mutants of bacteriophage P2. Mol. Gen. Genet. **128**:249–260.
33. **Luftig, R. B., W. B. Wood, and R. Okinaka.** 1971. Bacteriophage T4 head morphogenesis: on the nature of gene 49-defective heads and their role as intermediates. J. Mol. Biol. **57**:555–573.
34. **Mural, R. J., R. J. Chesney, D. Vapnek, M. M. Kropf, and J. R. Scott.** 1979. Isolation and characterization of cloned fragments of bacteriophage P1 DNA. Virology **93**:387–397.
35. **Onorato, L., and M. K. Showe.** 1975. Gene 21 protein-dependent proteolysis *in vitro* of purified gene 22 product of bacteriophage T4. J. Mol. Biol. **92**:395–412.
36. **Poteete, A. R., and J. King.** 1977. Functions of two new genes in *Salmonella* phage P22 assembly. Virology **76**:725–739.
37. **Ray, P., and H. Murialdo.** 1975. The role of gene Nu3 in bacteriophage lambda head morphogenesis. Virology **64**:247–263.
38. **Razza, R. B., C. A. Watkins, and J. R. Scott.** 1980. Phage P1 temperature-sensitive mutants with defects in the lytic pathway. Virology **105**:52–59.
39. **Scott, J. R.** 1968. Genetic studies on bacteriophage P1. Virology **36**:564–574.
40. **Showe, M. K., and L. W. Black.** 1973. Assembly core of bacteriophage T4: an intermediate in head formation. Nature (London) New Biol. **242**:70–75.
41. **Showe, M. K., and E. Kellenberger.** 1975. Control mechanisms in virus assembly, p. 407–438. *In* D. C. Burke and W. C. Russel (ed.), Control processes in virus multiplication. Cambridge University Press, Cambridge, England.
42. **Simon, L.** 1972. Infection of *Escherichia coli* by T2 and T4 bacteriophages as seen in the electron microscope: T4 head morphogenesis. Proc. Natl. Acad. Sci. U.S.A. **69**:907–911.
43. **Sternberg, N.** 1979. A characterization of bacteriophage P1 DNA fragments cloned in a λ vector. Virology **96**:129–

142.
44. **Sternberg, N., D. Hamilton, S. Austin, M. Yarmolinsky, and R. Hoess.** 1981. Site-specific recombination and its role in the life cycle of bacteriophage P1. Cold Spring Harbor Symp. Quant. Biol. **45**:297–309.
45. **Toussaint, A., N. Lefebre, J. R. Scott, J. A. Cowan, F. de Bruijn, and A. I. Bukhari.** 1978. Relationships between temperate phages Mu and P1. Virology **89**:146–161.
46. **van de Putte, P., S. Cramer, and M. Giphart-Gassler.** 1980. Invertible DNA determines host specificity of bacteriophage Mu. Nature (London) **286**:218–222.
47. **Walker, D. H., Jr., and T. F. Anderson.** 1970. Morphological variants of coliphage P1. J. Virol. **5**:765–782.
48. **Walker, D. H., Jr., and J. T. Walker.** 1975. Genetic studies of coliphage P1. I. Mapping by use of prophage deletions. J. Virol. **16**:525–534.
49. **Walker, D. H., Jr., and J. T. Walker.** 1976. Genetic studies of coliphage P1. III. Extended genetic map. J. Virol. **20**:177–187.
50. **Walker, J. T., and D. H. Walker, Jr.** 1980. Mutations in coliphage P1 affecting host cell lysis. J. Virol. **35**:519–530.
51. **Walker, J. T., and D. H. Walker, Jr.** 1981. Structural proteins of coliphage P1, p. 69–77. *In* M. S. DuBow (ed.), Progress in clinical biological research, vol. 64. Alan R. Liss, Inc., New York.
52. **Ward, S., R. B. Luftig, J. H. Wilson, H. Eddleman, H. Lyle, and W. B. Wood.** 1970. Assembly of bacteriophage T4 tail fibers. II. Isolation and characterization of tail fiber precursors. J. Mol. Biol. **54**:15–31.
53. **Wood, W. B., and J. King.** 1979. Genetic control of complex bacteriophage assembly. Compr. Virol. **13**:581–633.
54. **Wood, W. B., and H. R. Revel.** 1976. The genome of bacteriophage T4. Bacteriol. Rev. **40**:847–868.
55. **Yanagida, M., and C. Ahmad-Zadeh.** 1970. Determination of gene product positions in bacteriophage T4 by specific antibody association. J. Mol. Biol. **51**:411–421.
56. **Yanagida, M., E. Boy de la Tour, C. Alff-Steinberger, and E. Kellenberger.** 1970. Studies on the morphopoiesis of the head of bacteriophage T-even. VIII. Multilayered polyheads. J. Mol. Biol. **50**:35–58.
57. **Yarmolinsky, M.** 1982. Bacteriophage P1, p. 34–43. *In* S. J. O'Brien (ed.), Genetic maps, vol. 2. National Cancer Institute, Bethesda, Md.